Three-Dimensional Wigner-Function Description of the Quantum Free-Electron Laser

N. Piovella,[1,2] M. M. Cola,[1,2] L. Volpe,[1,2] A. Schiavi,[3] and R. Bonifacio[2,4]

[1]*Dipartimento di Fisica, Università Degli Studi di Milano, via Celoria 16, I-20133 Milano, Italy*
[2]*INFN - sezione di Milano - via Celoria 16, I-20133 Milano, Italy*
[3]*Dipartimento di Energetica, Università di Roma "La Sapienza" and INFN, Via Scarpa 14, I-00161 Roma, Italy*
[4]*Centro Brasileiro de Pesquisas Físicas, Rio de Janeiro, Brazil*

(Received 15 May 2007; published 29 January 2008)

A free-electron laser (FEL) operating in the quantum regime can provide a compact and monochromatic x-ray source. Here we present the complete quantum model for a FEL with a laser wiggler in three spatial dimensions, based on a discrete Wigner-function formalism taking into account the longitudinal momentum quantization. The model describes the complete spatial and temporal evolution of the electron and radiation beams, including diffraction, propagation, laser wiggler profile and emittance effects. The transverse motion is described in a suitable classical limit, since the typical beam emittance values are much larger than the Compton wavelength quantum limit. In this approximation we derive an equation for the Wigner function which reduces to the three-dimensional Vlasov equation in the complete classical limit. Preliminary numerical results are presented together with parameters for a possible experiment.

DOI: 10.1103/PhysRevLett.100.044801 PACS numbers: 41.60.Cr, 05.30.−d, 42.50.Nn

The realization of a free-electron laser (FEL) in the self-amplified spontaneous emission (SASE) mode [1] is presently the goal of several projects, such as the LCLS [2] at Stanford, USA, and XFEL [3] in Hamburg, Germany, to obtain a high-brightness x-ray source. However, such sources will radiate a pulse with a broad spectrum composed by many random superradiant spikes [4]. Recently it has been shown that a FEL can operate in a quantum regime [5], in which the spiking behavior observed in the SASE mode disappears and the spectrum is composed by a single narrow line [6,7], providing a huge improvement in the coherence of SASE-FEL based x-ray sources. The transition from the classical to the quantum regime is controlled by the "quantum FEL parameter" $\bar{\rho} = \rho(mc\gamma_r/\hbar k_r)$ (where ρ is the FEL parameter [1]), equal to the ratio between the maximum classical momentum spread (of the order of $mc\gamma_r\rho$) and the photon recoil momentum $\hbar k_r$. It expresses also the maximum number of photons emitted per electron in the classical regime. When $\bar{\rho} \gg 1$ a SASE-FEL operates in the classical "multiphoton" regime, and the spectrum of the emitted field is broad and chaotic. Conversely, when $\bar{\rho} \leq 1$ each electron emits a single photon and the spectrum consists of a single line, whose width is Fourier limited by the electron beam duration [8].

For an experimental realization of a quantum free-electron laser (QFEL) it is necessary to use a laser wiggler instead of the usual magnetic wiggler [9]. Such a choice sets stringent conditions on the electron beam quality [8], which can be explored only by numerical simulations in three spatial dimensions (3D). In this Letter we extend the 1D Wigner model of QFEL [10] to a full 3D model with a laser wiggler, and we present preliminary results of the numerical code QFEL3D.

In QFEL [5,11], the electrons' system can be described by the Liouville–von Neumann equation $\partial\hat{\varrho}/\partial\bar{z} = i[\hat{H}, \hat{\varrho}]$ for the electron density operator $\hat{\varrho}$, where in the 1D limit the Hamiltonian operator is [12]:

$$\hat{H}(\bar{z}) = \frac{\hat{p}^2}{2\bar{\rho}^{3/2}} - i[A(\bar{z}, z_1)e^{i\hat{\theta}} - A^*(\bar{z}, z_1)e^{-i\hat{\theta}}]. \quad (1)$$

With a circularly polarized counterpropagating laser beam (laser wiggler) instead of the usual static wiggler, the variables and the parameters in Eq. (1) are defined as follows: $\theta = (k_r + k_L)z - c(k_r - k_L)t - \delta\bar{z}$ is the electron phase, where $k_L = 2\pi/\lambda_L$ and $k_r = 2\pi/\lambda_r$ are the laser and radiation wave numbers, respectively; $p = mc(\gamma - \gamma_0)/(\hbar k_r)$ is the longitudinal momentum, in units of the photon recoil momentum, $\hbar k_r$, and $\delta = mc(\gamma_0 - \gamma_r)/(\bar{\rho}\hbar k_r)$ is the detuning, where γ_0 and $\gamma_r = [\lambda_L(1 + a_0^2)/4\lambda_r]^{1/2}$ are the initial and resonant electron energy in mc^2 units, respectively; the position along the wiggler $\bar{z} = z/L_g$ is expressed in gain length units $L_g = \lambda_L/(8\pi\rho\sqrt{\bar{\rho}})$, and the electron position along the beam is $z_1 = (z - v_r t)/(\beta_r L_c)$, where $v_r = c\beta_r$ is the resonant velocity and $L_c = \lambda_r/(4\pi\rho\sqrt{\bar{\rho}})$ is the cooperation length; $\rho = (1/2\gamma_r)(I/I_A)^{1/3}(\lambda_L a_0/4\pi\sigma)^{2/3}$ is the classical FEL parameter, I is the beam peak current, $I_A \approx 17$ kA is the Alfvén current, σ is the transverse rms beam size; $a_0 = eE_0/mc^2k_L$ and E_0 is the laser electric field; A is the slowly varying amplitude of the radiation field, defined such that $|A|^2 = \epsilon_0|E_r|^2/(\hbar\omega_r n_b)$ is the average number of photons emitted per electron, E_r is the radiation electric field, $n_b = I/(2\pi\sigma^2 ec)$ is the electron density and $\omega_r = ck_r$. The operators associated with the electron position θ and momentum p are $\hat{\theta}$ and $\hat{p} = -i\partial/\partial\theta$, so that $[\hat{\theta}, \hat{p}] = i$. In this formalism $\bar{z}$ takes the role of the "time", whereas z_1 is the longitudinal coordinate in the electron rest frame and appears in Eq. (1) as a parametric dependence in the classical field amplitude A. The 1D discrete Wigner-function representation of the statistic operator $\hat{\varrho}$

is $W_n(\theta, \bar{z}; z_1) = w_n(\theta, \bar{z}; z_1) + \sum_{m\in\mathbb{Z}}[(-1)^{n-m-1}/(n - m - 1)\pi]w_{m+1/2}(\theta, \bar{z}; z_1)$ [13], where

$$w_s(\theta, \bar{z}; z_1) = \frac{1}{2\pi}\int_{-\pi}^{+\pi} d\theta' e^{-i2s\theta'}\langle\theta + \theta'|\hat{\varrho}(\bar{z}; z_1)|\theta - \theta'\rangle \tag{2}$$

and $s = n$ or $s = n + 1/2$, with $n, m \in \mathbb{Z}$. Notice that w_s has indexes both integer and half-integer, and w_n and $w_{n+1/2}$ are periodic functions of θ, with a period π and 2π, respectively. With these definitions, it has been shown that QFEL can be described in the 1D limit by the following equations [10]:

$$\frac{\partial w_s}{\partial \bar{z}} + \frac{s}{\bar{\rho}^{3/2}}\frac{\partial w_s}{\partial \theta} - [Ae^{i\theta} + A^* e^{-i\theta}]\{w_{s+1/2} - w_{s-1/2}\} = 0, \tag{3}$$

$$\frac{\partial A}{\partial \bar{z}} + \frac{\partial A}{\partial z_1} = \sum_{m=-\infty}^{+\infty}\int_{-\pi}^{+\pi} d\theta e^{-i\theta} w_{m+1/2} + i\delta A. \tag{4}$$

Notice that the momentum quantization appears in Eq. (3) as a finite difference in the interaction term with the electromagnetic field.

The 1D FEL Wigner model of Eqs. (3) and (4) can be conveniently extended to a three-dimensional description of the electron and field dynamics. Classically, a 3D analysis of FELs is accomplished either by tracking the macroparticle trajectories in the self-consistent fields and then calculating the bunching term in the field equation by averaging over the electrons [14], or by solving the Vlasov-Maxwell equations for the electron distribution and the field amplitude [15]. In the quantum description, the evolution of the electron density operator $\hat{\varrho}$ is determined by the following 3D Hamiltonian operator:

$$\hat{H}(\bar{z}) = \frac{\hat{p}^2}{2\bar{\rho}^{3/2}} + \frac{\alpha b}{2}\hat{p}_t^2 + \left[\frac{\xi}{2\rho\sqrt{\bar{\rho}}}(1 - |g(\hat{\bar{\mathbf{x}}}_t, \bar{z})|^2) - \frac{bX}{4}\alpha^2\hat{p}_t^2\right]\hat{p} - i[g^*(\hat{\bar{\mathbf{x}}}_t, \bar{z})A(\hat{\bar{\mathbf{x}}}_t, \bar{z}, z_1)e^{i\hat{\theta}} - \text{H.c.}] + \frac{\xi}{\alpha\rho\sqrt{\bar{\rho}}X}|g(\hat{\bar{\mathbf{x}}}_t, \bar{z})|^2. \tag{5}$$

This expression extends the 1D operator (1) by including the transverse electron dynamics and the field and laser wiggler spatial dependence. The transverse momentum operator $\hat{\mathbf{p}}_t = -i\nabla_{\bar{\mathbf{x}}_t}$ is associated with the variable $\mathbf{p}_t = (\gamma_r\sigma/\lambda\!\!\!^{-}_c)\mathbf{x}_t'$ (where $\mathbf{x}_t' = d\mathbf{x}_t/dz$ and $\lambda\!\!\!^{-}_c = \hbar/mc$ is the Compton wavelength), and it is canonically conjugated to the transverse position operator $\hat{\bar{\mathbf{x}}}_t = \hat{\mathbf{x}}_t/\sigma$, with commutation rules $[\hat{\bar{x}}_x, \hat{p}_x] = [\hat{\bar{x}}_y, \hat{p}_y] = i$. The parameters appearing in Eq. (5) are $\alpha = \lambda\!\!\!^{-}_c/\epsilon_n$, where ϵ_n is the normalized beam transverse emittance, $X = 4\pi\epsilon_n/(\gamma_r\lambda_r)$, $\xi = a_0^2/(1 + a_0^2)$ and $b = L_g/\beta^*$, where $\beta^* = \sigma^2\gamma_r/\epsilon_n$. In Eq. (5) the second term $(\alpha b/2)\hat{p}_t^2 = -L_g(\lambda\!\!\!^{-}_c/2\gamma_r)\nabla_{\bar{\mathbf{x}}_t}^2$ is the transverse kinetic energy, the third term describes the change of the FEL resonance due to variation of the laser wiggler profile and to beam angular spread. The transverse laser wiggler amplitude profile is described by $g(\bar{\mathbf{x}}_t, \bar{z})$ (equal to unity in the 1D model) and, for a TEM_{00} Gaussian mode, it can be written as

$$g(\bar{\mathbf{x}}_t, \bar{z}) = \frac{1}{[1 - id(\bar{z} - \bar{z}_0)]}\exp\left\{\frac{-|\bar{\mathbf{x}}_t|^2}{4\sigma_L^2[1 - id(\bar{z} - \bar{z}_0)]}\right\}, \tag{6}$$

where $\sigma_L = R/\sigma$, $d = L_g/Z_L$, $Z_L = 4\pi R^2/\lambda_L$, and R is the minimum rms laser radius at the beam waist position $\bar{z}_0$. In the 3D description, the Wigner functions (2) are extended to include the transverse dynamics:

$$w_s(\theta, \bar{\mathbf{x}}_t, \mathbf{p}_t, \bar{z}; z_1) = \frac{1}{2\pi^3}\int_{-\pi}^{+\pi} d\theta' \int d^2\bar{\mathbf{x}}_t' e^{-i2(s\theta' + \bar{\mathbf{x}}_t'\cdot\mathbf{p}_t)}\langle\theta + \theta', \bar{\mathbf{x}}_t + \bar{\mathbf{x}}_t'|\hat{\varrho}|\bar{\mathbf{x}}_t - \bar{\mathbf{x}}_t', \theta - \theta'\rangle, \tag{7}$$

where s is integer or half-integer. Tracing the Wigner function over one variable, we obtain the probability distribution for the other variables. In particular, the momentum distribution is $P_m(\mathbf{p}_t, \bar{z}; z_1) = \int_{-\pi}^{+\pi} d\theta \int d^2\bar{\mathbf{x}}_t w_m(\theta, \bar{\mathbf{x}}_t, \mathbf{p}_t, \bar{z}; z_1)$, and the position distribution is $Q(\theta, \bar{\mathbf{x}}_t, \bar{z}; z_1) = \sum_m \int d^2\mathbf{p}_t\{w_m(\theta, \bar{\mathbf{x}}_t, \mathbf{p}_t, \bar{z}; z_1) + w_{m+1/2}(\theta, \bar{\mathbf{x}}_t, \mathbf{p}_t, \bar{z}; z_1)\}$. Note that the half-integer functions $w_{m+1/2}$ do not contribute to the integral in P_m [13]. As a consequence, $\sum_m \int_{-\pi}^{+\pi} d\theta \int d^2\mathbf{p}_t w_m(\theta, \bar{\mathbf{x}}_t, \mathbf{p}_t, \bar{z}; z_1) = J(\bar{\mathbf{x}}_t, \bar{z}; z_1)$ is the current density (normalized to unity at the peak) and $\int d^2\bar{\mathbf{x}}_t J(\bar{\mathbf{x}}_t, \bar{z}; z_1) = I_0(z_1)$ is the stationary longitudinal beam profile [7].

Differentiating Eq. (7) and inserting it in the Liouville–von Neumann equation for $\hat{\varrho}$ with the Hamiltonian operator of Eq. (5), with long but standard procedures we have obtained the exact evolution equation for the Wigner function w_s (which will be published in a more extended paper). This equation describes an electron beam with any transverse normalized emittance, down to the Compton wavelength quantum limit. However, here we are interested in describing an electron beam in which the transverse momentum distribution is thermal, with a width $\Delta x' \sim \epsilon_n/(\sigma\gamma_r)$ much larger than the quantum limit $\lambda\!\!\!^{-}_c/(\sigma\gamma_r)$ of an ultracold beam with normalized emittance $\epsilon_n \sim \gamma_r\Delta x\Delta x' \sim \lambda\!\!\!^{-}_c$ (i.e., limited by the Heisenberg Uncertainty Principle only, $\Delta x\Delta p_x \sim \hbar$, with $\Delta p_x \sim mc\gamma_r\Delta x'$ and $\Delta x \sim \sigma$). To this purpose, we have introduced the dimensionless transverse momentum $\bar{\mathbf{p}}_t = (\sigma\gamma_r/\epsilon_n)\mathbf{x}_t' = \alpha\mathbf{p}_t$ and performed a series expansion in powers of α in the exact motion equation for w_s. Then, since typical values of α are of the order of 10^{-6}, we can keep only zero-order terms in α obtaining the following equations for $w_s(\theta, \bar{\mathbf{x}}_t, \bar{\mathbf{p}}_t, \bar{z}; z_1)$ and $A(\bar{\mathbf{x}}_t, \bar{z}, z_1)$:

$$\frac{\partial w_s}{\partial \bar{z}} + b\bar{\mathbf{p}}_t \cdot \nabla_{\bar{\mathbf{x}}_t} w_s + \left\{\frac{s}{\bar{\rho}^{3/2}} + \frac{\xi}{2\rho\sqrt{\bar{\rho}}}(1-|g|^2) - \frac{b^2}{4a}\bar{p}_t^2\right\} \times \frac{\partial w_s}{\partial \theta} - (g^* A e^{i\theta} + \text{c.c.})[w_{s+1/2} - w_{s-1/2}] - \frac{\xi}{\rho\sqrt{\bar{\rho}}X}\nabla_{\bar{\mathbf{x}}_t}|g|^2 \cdot \nabla_{\bar{\mathbf{p}}_t} w_s = 0, \quad (8)$$

$$\frac{\partial A}{\partial \bar{z}} + \frac{\partial A}{\partial z_1} - ia\nabla^2_{\bar{\mathbf{x}}_t} A = g\sum_m \int d^2\bar{\mathbf{p}}_t \int_{-\pi}^{+\pi} d\theta e^{-i\theta} w_{m+1/2} + i\delta A. \quad (9)$$

In Eq. (9) $a = L_g/Z_r = b/X$ is the diffraction parameter and $Z_r = 4\pi\sigma^2/\lambda$ is the Rayleigh range of the emitted radiation with a transverse radius equal to the electron beam radius.

It is important to note that Eq. (8) reduces to a Vlasov equation in the classical limit $\bar{\rho} \gg 1$. In fact, switching to the classical FEL scaling (i.e., $A = \sqrt{\bar{\rho}}A_c$, $\bar{z} = \sqrt{\bar{\rho}}\bar{z}_c$, $z_1 = \sqrt{\bar{\rho}}z_{1c}$, $\delta = \delta_c/\sqrt{\bar{\rho}}$, $b = b_c/\sqrt{\bar{\rho}}$ and $a = a_c/\sqrt{\bar{\rho}}$, see [12]), for $\bar{\rho} \to \infty$ the new longitudinal momentum, $\bar{p} = s/\bar{\rho}$, can be treated as a continuous variable and $w_s(\theta, \bar{\mathbf{x}}_t, \bar{\mathbf{p}}_t, \bar{z}; z_1) \to \bar{\rho} f(\theta, \bar{p}, \bar{\mathbf{x}}_t, \bar{\mathbf{p}}_t, \bar{z}_c; z_{1c})$, where f is a classical electron distribution function. In this limit, Eqs. (8) and (9) reduce to the classical Vlasov-Maxwell equations:

$$\frac{\partial f}{\partial \bar{z}_c} + b_c\bar{\mathbf{p}}_t \cdot \nabla_{\bar{\mathbf{x}}_t} f + \left\{\bar{p} + \frac{\xi}{2\rho}(1-|g|^2) - \frac{b_c^2}{4a_c}\bar{p}_t^2\right\}\frac{\partial f}{\partial \theta} - (g^* A_c e^{i\theta} + \text{c.c.})\frac{\partial f}{\partial \bar{p}} - \frac{\xi}{\rho X}(\nabla_{\bar{\mathbf{x}}_t}|g|^2) \cdot \nabla_{\bar{\mathbf{p}}_t} f = 0, \quad (10)$$

$$\frac{\partial A_c}{\partial \bar{z}} + \frac{\partial A_c}{\partial z_1} - ia_c\nabla^2_{\bar{\mathbf{x}}_t} A_c = g\int_{-\pi}^{+\pi} d\theta \int_{-\infty}^{+\infty} d\bar{p} \int d^2\bar{\mathbf{p}}_t e^{-i\theta} f + i\delta_c A_c. \quad (11)$$

The quantum evolution for w_s, Eq. (8), contains the quantization of the longitudinal momentum in units of $\hbar k$ (as the 1D model) and describes the transverse dynamics by terms completely analogue to those appearing in the Vlasov Eq. (10). In particular, the second term in Eq. (8), $b\bar{\mathbf{p}}_t \cdot \nabla_{\bar{\mathbf{x}}_t}$, corresponds, with unscaled variables, to $\mathbf{x}_t' \cdot \nabla$ and describes the transverse drift of the beam, responsible for the beam section increasing from the waist position $\bar{z}_0$ as $\sigma(z) = \sigma\sqrt{1 + [(z - z_0)/\beta^*]^2}$ in the free space and for a Gaussian beam. The second and third terms in the curl parenthesis in Eq. (8) account for the change of the FEL resonance induced by the laser wiggler profile and by the beam emittance. In particular $(b^2/4a)\bar{p}_t^2 \sim (1/2\rho\sqrt{\bar{\rho}}) \times (\epsilon_n/\sigma)^2/(1 + a_0^2)$ if we assume that the maximum divergence angle is $|\mathbf{x}_t'| \sim \epsilon_n/\gamma_r\sigma$. The last term $-(\xi/\rho\sqrt{\bar{\rho}}X)(\nabla_{\bar{\mathbf{x}}_t}|g|^2) \cdot \nabla_{\bar{\mathbf{p}}_t}$ in Eq. (8) corresponds, with unscaled variables, to $\mathbf{x}_t'' \cdot \nabla_{\mathbf{x}_t'}$, where $\mathbf{x}_t'' = -(a_0^2/2\gamma_r^2) \times (\nabla_{\mathbf{x}_t}|g|^2)$ is the ponderomotive force due to the laser transverse gradient.

A numerical code QFEL3D has been developed for solving the coupled Eqs. (8) and (9) based on a Fourier decomposition of the Wigner function and on finite-difference integration of the motion equations on a Cartesian three-dimensional spatial grid. In the simulations the initial electron beam was described by a thermal state of energy $mc^2\gamma_0$ and transverse phase space distribution $w_0(\theta, \bar{\mathbf{x}}_t, \bar{\mathbf{p}}_t, 0; z_1) \propto \exp\{-|\bar{\mathbf{x}}_t + b\bar{z}_0\bar{\mathbf{p}}_t|^2/2 - |\bar{\mathbf{p}}_t|^2/2\}$, with the waist position at $\bar{z} = \bar{z}_0$. For simplicity, we did not include in the model the electrons' energy spread, which, however, can be taken into account by an inhomogeneous broadening in the equation for A, as it has been described in Ref. [16].

Here we present preliminary results for the quantum regime, $\bar{\rho} = 0.2$, in steady-state operation mode, i.e., neglecting z_1 dependence. Furthermore, we assume a uniform laser wiggler ($g = 1$), which can be realized using a laser with a flattened transverse profile. Such lasers can be produced by suitable transparency films [17] or by overlapping different Gaussian beams [18]. In both cases, it is possible to realize a laser which remains almost transversally flat within few Rayleigh ranges Z_L from the beam waist.

Assuming $g = 1$, the system depends on the diffraction and emittance parameters only, namely a and b. The interaction is over 10 gain lengths ($\bar{z}_{\max} = c\tau_{\text{int}}/L_g = 10$) and the beam waist is in the middle, $\bar{z}_0 = 5$. A set of

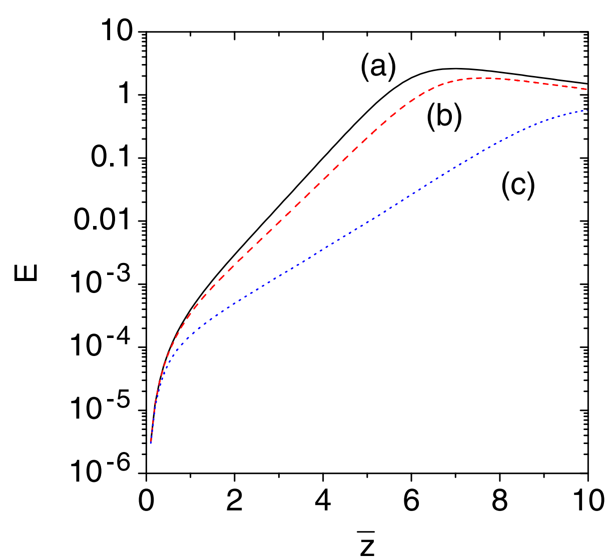

FIG. 1 (color online). Total radiated energy, $E(\bar{z}) = \int d^2\bar{\mathbf{x}}_t|A|^2$, vs $\bar{z}$ for $\bar{\rho} = 0.2$, $a = 1.6 \times 10^{-4}$, $g = 1$ and (a) $b = 0$ ($X = 0$), (b) $b = 0.014$ ($X = 88$), (c) $b = 0.028$ ($X = 176$). The electron beam focuses at $\bar{z}_0 = 5$.

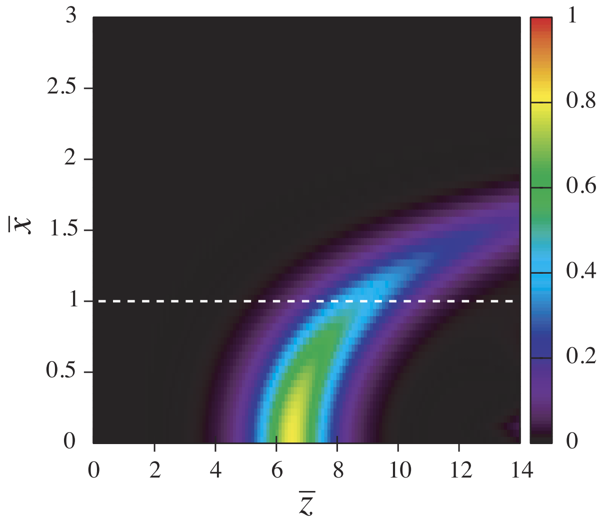

FIG. 2 (color online). Radiation intensity $|A|^2$ as a function of transverse coordinate $\bar{x}$ and of wiggler position $\bar{z}$. Parameters same as for curve (b) in Fig. 1. The dashed line corresponds to the electron beam rms radius σ. As a reference, the 1D model intensity would saturate to unity.

possible experimental parameters corresponding to the presented simulations is: $\lambda_r = 2$ Å, $\lambda_L = 1\ \mu$m, $\gamma_r = 36$, $I = 884$ A, $\sigma = 11.5\ \mu$m and $a_0 = 0.15$ (which could be realized for instance by a laser wiggler with power $P_L \sim 1$ TW, duration $\tau_L = 2\tau_{\rm int} = 88$ ps and Rayleigh range $Z_L = 6.7$ mm). The gain length is $L_g = 1.3$ mm, so that the diffraction parameter is $a = 1.6 \times 10^{-4}$. We have considered three different values of the beam emittance in order to investigate its effects on the gain: (a) $\epsilon_n = 0$, i.e., $b = X = 0$; (b) $\epsilon_n = 0.05$ mm-mrad, i.e., $b = 0.014$ and $X = 88$; (c) $\epsilon_n = 0.1$ mm-mrad, i.e., $b = 0.028$ and $X = 176$. Figure 1 shows the total FEL radiation energy, $E(\bar{z}) = \int d^2\bar{\mathbf{x}}_t |A|^2$, vs $\bar{z}$ for the cases (a)–(c). Figure 2 shows a color map of the intensity in the plane $(\bar{x}, \bar{z})$ for the (b) case. It can be seen that intensity saturates to a lower level in the beam halo with respect to the beam axis, and that the gain changes along the transverse direction. Notice that the total emitted energy and the on-axis peak intensity can reach a significant fraction of the 1D model for the proposed parameters (b).

In summary, we have proposed a novel 3D quantum model for a FEL with a laser wiggler, which takes into account transverse emittance and radiation diffraction effects as well as longitudinal propagation effects and the spatial profile of the laser wiggler field. The electron motion is described by a Wigner function, combining the classical transverse motion and the quantum longitudinal dynamics. Preliminary numerical results show that the detrimental effect of the emittance on the gain does not prevent for an exponential amplification of the radiation with reasonable experimental parameters. Further studies are required to investigate in detail the effects of the spatial variation of the laser wiggler intensity and the 3D dynamics of the SASE mode operation.

R. B. acknowledges partial support from The National Council of Scientific and Technological Development (Brasil).

[1] R. Bonifacio, C. Pellegrini, and L. Narducci, Opt. Commun. **50**, 373 (1984).

[2] The LCLS Design Study Group, SLAC, LCLS Design Study Report No. SLAC-R521, Stanford, 1998; http://www-ssrl.slac.stanford.edu/lcls/CDR.

[3] M. Altarelli *et al.*, The European X-Ray Free-Electron Laser: Technical design report, DESY 2006-097 July 2007; http://xfel.desy.de/tdr.

[4] R. Bonifacio, L. De Salvo, P. Pierini, N. Piovella, and C. Pellegrini, Phys. Rev. Lett. **73**, 70 (1994).

[5] R. Bonifacio, M. M. Cola, N. Piovella, and G. R. M. Robb, Europhys. Lett. **69**, 55 (2005).

[6] R. Bonifacio, N. Piovella, G. R. M. Robb, Nucl. Instrum. Methods Phys. Res., Sect. A **543**, 645 (2005).

[7] R. Bonifacio, N. Piovella, G. R. M. Robb, and A. Schiavi, Phys. Rev. ST Accel. Beams **9**, 090701 (2006).

[8] R. Bonifacio, N. Piovella, M. M. Cola, and L. Volpe, Nucl. Instrum. Methods Phys. Res., Sect. A **577**, 745 (2007).

[9] R. Bonifacio, Nucl. Instrum. Methods Phys. Res., Sect. A **546**, 634 (2005); R. Bonifacio, M. Ferrario, G. R. M. Robb, N. Piovella, A. Schiavi, and L. Serafini, *Proceedings of the 27th International Free Electron Laser Conference* (FEL 2005, Stanford, CA), Vol 71.

[10] R. Bonifacio, M. M. Cola, R. Gaiba, L. Volpe, N. Piovella, and A. Schiavi, Opt. Commun. **274**, 347 (2007).

[11] G. Preparata, Phys. Rev. A **38**, 233 (1988).

[12] In this Letter we adopt the quantum FEL scaling (see Ref. [5]) instead of the usual classical scaling of Ref. [1]. In the quantum scaling, $\bar{\rho}$ does not appear explicitly in the solution of the quantum regime, but it is contained in the definition of the variables.

[13] J. P. Bizarro, Phys. Rev. A **49**, 3255 (1994).

[14] N. M. Kroll, P. L. Morton, and M. N. Rosenbluth, IEEE J. Quantum Electron. **17**, 1436 (1981).

[15] Y. H. Chin, K. J. Kim, and M. Xie, Phys. Rev. A **46**, 6662 (1992).

[16] N. Piovella and R. Bonifacio, Nucl. Instrum. Methods Phys. Res., Sect. A **560**, 240 (2006).

[17] F. Gori, Opt. Commun. **107**, 335 (1994); V. Bagini *et al.*, J. Opt. Soc. Am. A **13**, 1385 (1996).

[18] A. A. Tovar, J. Opt. Soc. Am. A **18**, 1897 (2001).